

Improvement of mechanical-antibacterial performances of AR/PMMA with TiO₂ and HPQM treated by N-2(aminoethyl)-3-aminopropyl trimethoxysilane

Journal:	<i>Journal of Reinforced Plastics and Composites</i>
Manuscript ID	JRP-20-0775.R1
Manuscript Type:	Original Article
Date Submitted by the Author:	n/a
Complete List of Authors:	Tangudom, Paveena; King Mongkut's University of Technology Thonburi, Materials Technology Martin-Fabiani, Ignacio ; Loughborough University, Department of Materials Prapagdee, Benjaphorn; Mahidol University Faculty of Environment and Resource Studies, Laboratory of Environmental Biotechnology Markpin, Teerasak; King Mongkut's University of Technology Thonburi, Materials Technology Wimolmala, Ekachai; KMUTT, Materials Technology Sombatsompop, Narongrit; KMUTT, Materials Technology; KMUTT,
Keyword:	Acrylic rubber, Antibacterial performance, Poly (methyl methacrylate), Silane coupling agent, Titanium dioxide
Abstract:	The mechanical and antibacterial properties of acrylic rubber/poly(methyl methacrylate) (AR/PMMA) blend at 10 to 50 wt% of AR content with non-treated and treated titanium dioxide (TiO ₂) and 2-Hydroxypropyl-3-piperazinyl-quinoline carboxylic acid methacrylate (HPQM) by N-2(aminoethyl)-3-aminopropyl trimethoxysilane were studied. The antibacterial property against Escherichia coli was evaluated. The results found that the mechanical properties of ART-TiO ₂ /PMMA and ART-HPQM/PMMA blend were higher than that of the ARTiO ₂ /PMMA and ARHPQM/PMMA blend. For antibacterial property, the ARHPQM/PMMA and ART-HPQM/PMMA blend could act as the antibacterial material, while the ARTiO ₂ /PMMA blend did not show. However, the ART-TiO ₂ /PMMA blend could inhibit bacterial cell growth with 10 to 30 wt% of AR content. The recommended compositions of ART-TiO ₂ /PMMA blend, which improved both mechanical and antibacterial properties, were 10 to 30 wt% of AR and were 10 to 50 wt% of AR for ART-HPQM/PMMA. Moreover, the UV radiation increased the antibacterial properties by the destruction of the interaction in treated TiO ₂ and HPQM and improved the antibacterial performance of ART-TiO ₂ /PMMA and ART-HPQM/PMMA blend.

Revised JRP-20-775

Improvement of mechanical-antibacterial performances of AR/PMMA
with TiO₂ and HPQM treated by N-2(aminoethyl)-3-aminopropyl
trimethoxysilane

Paveena Tangudom^a, Ignacio Martín-Fabiani^b, Benjaphorn Prapagdee^c,
Ekachai Wimolmala^a, Teerasak Markpin^a and Narongrit Sombatsompop^{a,*}

^a Polymer PROcessing and Flow (P-PROF) Research Group, Materials Technology Program, School
of Energy, Environment and Materials, King Mongkut's University of Technology Thonburi
(KMUTT), 126 Pracha-Uthit, Thungkru, Bangmod, Bangkok 10140, Thailand

^bDepartment of Materials, Loughborough University, Loughborough LE11 3TU, Leicestershire
United Kingdom

^cLaboratory of Environmental Biotechnology, Faculty of Environment and Resource Studies, Mahidol
University, Salaya, Phutthamonthon, Nakhon Pathom 73170, Thailand

*Correspondence to: Narongrit Sombatsompop; E-mail: narongrit.som@kmutt.ac.th
Tel.: +66 2 470-8645; Fax: +66 2 470-8647

ABSTRACT

The mechanical and antibacterial properties of acrylic rubber/poly(methyl methacrylate) (AR/PMMA) blend at 10 to 50 wt% of AR content with non-treated and treated titanium dioxide (TiO_2) and 2-Hydroxypropyl-3-piperazinyl-quinoline carboxylic acid methacrylate (HPQM) by N-2(aminoethyl)-3-aminopropyl trimethoxysilane were studied. The antibacterial property against *Escherichia coli* was evaluated. The results found that the mechanical properties of $\text{AR}^{\text{t-TiO}_2}$ /PMMA and $\text{AR}^{\text{t-HPQM}}$ /PMMA blend were higher than that of the AR^{TiO_2} /PMMA and AR^{HPQM} /PMMA blend. For antibacterial property, the AR^{HPQM} /PMMA and $\text{AR}^{\text{t-HPQM}}$ /PMMA blend could act as the antibacterial material, while the AR^{TiO_2} /PMMA blend did not show. However, the $\text{AR}^{\text{t-TiO}_2}$ /PMMA blend could inhibit bacterial cell growth with 10 to 30 wt% of AR content. The recommended compositions of $\text{AR}^{\text{t-TiO}_2}$ /PMMA blend, which improved both mechanical and antibacterial properties, were 10 to 30 wt% of AR and were 10 to 50 wt% of AR for $\text{AR}^{\text{t-HPQM}}$ /PMMA. Moreover, the UV radiation increased the antibacterial properties by the destruction of the interaction in treated TiO_2 and HPQM and improved the antibacterial performance of $\text{AR}^{\text{t-TiO}_2}$ /PMMA and $\text{AR}^{\text{t-HPQM}}$ /PMMA blend.

KEYWORDS: Acrylic rubber; Antibacterial performance; HPQM; Poly (methyl methacrylate); Silane coupling agent; Titanium dioxide

ABBREVIATIONS

AR^{TiO_2} /PMMA = AR/PMMA blend with non-treated TiO_2

AR^{HPQM} /PMMA = AR/PMMA blend with non-treated HPQM

$\text{AR}^{\text{t-TiO}_2}$ /PMMA = AR/PMMA blend with treated TiO_2

$\text{AR}^{\text{t-HPQM}}$ /PMMA = AR/PMMA blend with treated HPQM

1
2
3
4
5
6
7
8
9
10
11
12
13
14
15
16
17
18
19
20
21
22
23
24
25
26
27
28
29
30
31
32
33
34
35
36
37
38
39
40
41
42
43
44
45
46
47
48
49
50
51
52
53
54
55
56
57
58
59
60

Introduction

The toughened PMMA was produced by the addition with elastomer, including acrylic rubber (AR) (An et al., 2014; Lee et al., 2015), acrylonitrile butadiene styrene (ABS) (Haddadi et al., 2016), epoxidized natural rubber (ENR) (Nakason et al., 2004), and poly(acrylonitrile-co-styrene) (ASA) (Cocco et al., 2013). The rubber phase adsorbed the impact energy and generated the plastic deformation in the polymer blend, resulting in the toughness of PMMA (Wang, Zhang, et al., 2019). The toughened PMMA can be used more widely than PMMA. The products from toughened PMMA, such as shower cabin, the cover sheet for sanitaryware, are often at risk of the bacteria accumulation on their surface. Therefore, the various additives, including titanium dioxide (TiO₂) (Alrahlah et al., 2018; Shen et al., 2019; Sodagar et al., 2016), zinc oxide (ZnO) (Sathya et al., 2019), chitosan (Tan et al., 2012), and 2-hydroxypropyl-3-piperazinyl-quinoline carboxylic acid methacrylate (HPQM) (Tangudom et al., 2019), are needed in order to extend this application. HPQM is a inorganic antibacterial agent, which is nontoxic to the human body and non-endocrine disruptor. HPQM could inhibit the cell wall synthesis and the DNA synthesis, resulting in cell death (Microsciencetech, 2000). Our previous study (Tangudom et al., 2018) found that the mechanical properties of the AR^{TiO₂}/PMMA blend decreased with increasing TiO₂ content due to the attraction between TiO₂ aggregation by the van der Waals force. Studies have pointed out significant problems, including the reduced mechanical properties of AR/PMMA by the TiO₂ agglomeration. Therefore, the diminished TiO₂ agglomeration by surface treatment with the silane coupling agents was interested.

Silane coupling agents consist of the silica atom and functional group, which could interact with the both organic and inorganic components. Their functional group interacts with the hydroxyl group on the TiO₂ surface (Ambrósio et al., 2016; Wang, Jiang, et al., 2019; Xiao et al., 2017). It developed the interaction between the polymer and TiO₂ particles and generated

the crosslinked interphase region (Sombatsompop & Chaochanchaikul, 2005). Work by Xiao et al. (2017) studied poly (dodecafluoroheptyl methacrylate) (PDFMA) filled with non-treated and treated TiO_2 by 3-(trimethoxysilyl) propylmethacrylate. The results found that the dispersibility of treated TiO_2 in PDFMA was better than that of the non-treated TiO_2 due to the chemical interaction between treated TiO_2 and PDFMA. The chemical interaction between TiO_2 and silane coupling agent was investigated by Zhao et al. (2012), who claimed that the TiO_2 and silane coupling agent could interact with each other through Ti-O-Si bonding. Occurrences of the good dispersibility and chemical bonding of treated TiO_2 was claimed to improve the mechanical properties of the matrix. This claim was in good agreement with findings of Ambrósio et al. (2016), found that the treated TiO_2 increased the mechanical properties of Polyamide11 (PA11) due to the improvement of the interfacial adhesion. Regarding the effect of antibacterial property, the non-treated TiO_2 could generate the reactive oxygen species (ROS), producing O_2^- , HOO^\bullet , and HO^\bullet in dark environment and HO^\bullet in UV environment (Gali et al., 2016). However, the effect of silane coupling agent on the mechanical and antibacterial properties of HPQM in the matrix is still not investigate.

Based on the literature review, the TiO_2 particles have the hydroxyl group on their surface, which increased the TiO_2 agglomeration. The TiO_2 agglomeration caused stress concentration and reduced the performance of ROS generation, resulting in the reduction of mechanical and antibacterial properties. In the case of HPQM, according to our previous work (Tangudom et al., 2019), the functional group could interfere with the miscibility of the AR and PMMA phase and decreased the mechanical property. Thus, the aim of this present study was to enhance the mechanical and antibacterial properties of the AR/PMMA blend filled with the surface treatment of TiO_2 and HPQM by N-2(aminoethyl)-3-aminopropyl trimethoxysilane or KBM603. As recommended by the previous study (Tangudom et al., 2018, 2019), the non-treated and treated of TiO_2 and HPQM content blend was fixed at 1.5 parts per

hundred (pph) in AR/PMMA blend and incorporated with AR phase for 10 to 50 wt%. The tensile properties and impact strength of AR/PMMA blend with non-treated and treated TiO₂ and HPQM were investigated. The antibacterial performance against *Escherichia coli* (ATCC 25922) was evaluated using the standard method of JIS Z2801:2010. The effect of UV radiation exposure on the antibacterial performance was recognized.

Materials and methods

Chemicals and materials

Acrylic rubber (AR) grade AR 71 and poly (methyl methacrylate) (PMMA) grade MD001 were supplied from Zeon Chemicals (Thailand) Co., Ltd. and Mitsubishi Rayon Co., Ltd., respectively. The rutile titanium dioxide (TiO₂) particles acts as a carrier and an antibacterial agent with an average primary particle size of 11.2 µm which was acquired from Chanjao Longevity Co., Ltd. A 2-hydroxypropyl-3-piperazinyl-quinoline carboxylic acid methacrylate (HPQM) grade BA 101 as an antibacterial agent was kindly provided from Koventure Co., Ltd. (10 wt% of HPQM in solution) (Microsciencetech, 2000). N-2(aminoethyl)-3-aminopropyl trimethoxysilane (Mw = 222.4) was used as the silane coupling agent for TiO₂ and HPQM, which applied from Shin-Etsu Chemical, Japan. The antibacterial agents were treated by the silane coupling agent called N-2(aminoethyl)3-aminopro-propyl trimethoxysilane (KBM603), which was supplied by Shin- Etsu Chemical Co., Ltd. (Tokyo).

Preparation treated TiO₂ and HPQM by the silane coupling agent

TiO₂ particles were cleaned by sonication in deionized water for an hour to break up any weakly flocculated particles and then dried in a hot-air oven at 60°C for 24 h. After that, the TiO₂ and HPQM (10 wt% of HPQM in water) were added to a 1 wt% of KBM603 in toluene

124 for 1 h and then dried at 60 °C for 48 h. Then, the solution, as called a treated TiO₂ and treated
125 HPQM was stirred at room temperature for 4 h at 50 °C.

126 *Specimen preparation*

127 The blends were prepared by mixing acrylic rubber with non-treated and treated of TiO₂
128 and HPQM at 1.5 parts per hundred (pph), which was called “modified AR”. The modified AR
129 compounds at loadings from 10 to 50 wt% were then blended with PMMA via a melt blending
130 process using a twin-screw extruder at a mixing temperature of 200 to 230 °C. The material
131 formulas are given in **Table 1**. Sheets of the blends for antibacterial performance testing were
132 prepared using a hot compression molding at an operating temperature of 230 °C, a holding
133 pressure of 15 N/mm², and an operating time of 15 min. The sheets had a thickness of
134 approximately 2 mm. Sheets of the blends for mechanical properties testing were prepared
135 using an injection molding machine. The samples were a dumbbell shape according to the
136 ISO 527-2:1993 standard.

137 *UV radiation exposure*

138 The rectangle samples of the AR^t-TiO₂/PMMA and AR^t-HPQM/PMMA blends were
139 exposed to UV radiation for 24 h using a QUV accelerated-weathering tester (Q-LAB,
140 Westlake, USA), in accordance with the ISO 4892-3:2016 standard procedure. The wavelength
141 of UV-A was 320–400 nm with an intensity of 0.77 W/m²/nm at 50 °C. These samples were
142 tested the antibacterial performance.

143 *Mechanical properties*

144 The mechanical properties, including impact strength, tensile toughness, tensile
145 modulus, tensile strength, and elongation at break of the AR/PMMA blends with non-treated
146 and treated of TiO₂ and HPQM were tested. The notched impact strength was measured using

1
2
3 147 a pendulum impact tester (5 joule) (HIT-5J, ZwickRoell, Germany), following the
4
5 148 ISO 179-1:2010 standard test method. Tensile testing was conducted according to the
6
7
8 149 ISO 527-2:1993 standard using a universal testing machine (Model H50kS, Tinius Olsen, UK).
9
10 150 The testing conditions were a gauge length of 50 mm and a crosshead speed of 50 mm/min. At
11
12 151 least five replicates were averaged for the reported value.
13
14

15 152 ***Qualitative and quantitative determination of antibacterial performance***
16
17
18

19 153 The antibacterial performance of non-treated and treated TiO₂ and HPQM of
20
21 154 AR/PMMA before and after UV radiation exposure against *Escherichia coli* (ATCC 25922)
22
23 155 was evaluated using the standard method of JIS Z2801:2010. The surface-sterilized specimens
24
25 156 (2.5×2.5 mm) were placed on sterilized Petri dishes. An inoculum of bacterial cell suspension
26
27 157 in Nutrient Broth (NB) at a cell turbidity of OD₆₀₀ ~ 0.1 was dropped onto the specimen surface
28
29 158 and then covered with sterilized polypropylene film. After incubation at 37 °C for 24 h, the
30
31 159 bacterial cell suspension on the specimen surface was washed with 10 mL of Soya Casein
32
33 160 Digest Lecithin Polysorbate (SCDLP) broth. Bacterial cell suspension in SCDLP was diluted
34
35 161 in 0.85% NaCl and the appropriate dilutions were spread on Nutrient Agar (NA) plates. After
36
37 162 incubation at 37 °C for 24 h, the number of bacterial colonies appearing on the NA plates from
38
39 163 the specimens with (N_i) and without TiO₂ addition (N₀) was counted. The values of
40
41 164 antibacterial activity (R) of the blends were calculated by the following equation (1) (Chung et
42
43 165 al., 2007).
44
45
46
47
48
49

50 166
$$\text{Antibacterial activity (R)} = \log \frac{N_0}{N_i} \quad (1)$$

51
52
53

54 167 A value of antibacterial activity (R value) which is equal to or higher than 2.0 indicates
55
56 168 greater than 99.9% bacterial reduction and the sample is accepted as an antibacterial material
57
58 169 according to the standard of JIS Z2801:2010.
59
60

Results and discussion

Mechanical properties of AR/PMMA blends filled with non-treated and treated TiO₂ and HPQM

Fig. 1 shows the tensile properties of the AR/PMMA and AR/PMMA blends with non-treated and treated TiO₂. **Fig. 1a** shows that the addition of non-treated TiO₂ decreased the tensile strength of the AR/PMMA blend at 10 and 20 wt% of AR contents and the effect was reverse at 30-50wt% of AR contents. The explanation of the decreased in tensile strength would be related to the interference of the non-treated TiO₂ on the interaction between AR and PMMA phases. PMMA and AR phases could be compatible due to the dipole-dipole interaction between the carbonyl group of PMMA and AR phase (Lommerse et al., 1998). **Fig. 2** shows the FTIR spectrum of PMMA, AR, and 50AR/PMMA blend. **Fig. 2a** shows the FTIR spectrum of PMMA. The peaks at 2962, 2951, 2844, 1141, 1190 and 1238 cm⁻¹ can be attributed to the stretching vibration mode of -CH₃, -C-H, -CH₂-, -O-CH₃, -C-O- and -C-O- (in carboxylic acid), respectively (Duan et al., 2008; Ramesh et al., 2007). The peaks at 1066, 986 and 841 cm⁻¹ are the characteristic absorption vibration of PMMA. The C-H bonded bending of CH₃ group is shows in peak at 1435 cm⁻¹ (Duan et al., 2008). The two peaks at 1387 and 754 cm⁻¹ can be assigned to the methylene group vibration (Duan et al., 2008). The peak at 1722 cm⁻¹ shows the presence of the acrylate carbonyl group (Ramesh et al., 2007). The FTIR spectrum of AR is presented in **Fig. 2b**. The peak at 2985 cm⁻¹ represent the C-H stretching vibration of OCH₂CH₃, while peak at 2934 represent the CH₂ stretching vibration of OCH₂CH₃ (Tangboriboon et al., 2008). Two peaks of 1446 and 1378 cm⁻¹ can be attributed to the CH₃ asymatic deformation of OCH₂CH₃ and the peaks at 1247 and 1152 cm⁻¹ represent C-O-C asymatric stretching vibration and R-C-O-R symmetric stretching vibration, respectively (Tangboriboon et al., 2009). Two peaks of 1096 and 1022

1
2
3 194 cm^{-1} can be assigned to skeletal vibration of acrylic acid (Tangboriboon et al., 2008). The peak
4
5 195 at 1726 cm^{-1} shows the presence of the carbonyl group (Kader & Bhowmick, 2000). However,
6
7 196 the functional groups of 50AR/PMMA blend similar to PMMA and AR, excepted the peak
8
9 197 represents the carbonyl group. It changed to 1725 cm^{-1} due to the weak bonding between
10
11 198 functional group. However, the change of proton of AR and PMMA was examined by the
12
13 199 chemical shift positions or δ values of ^1H -NMR spectrum.
14
15
16
17

18 200 **Fig. 3a-c** shows the ^1H -NMR spectrum of PMMA, AR, and 50AR/PMMA,
19
20 201 respectively. The assignments of peaks of protons and ^1H -NMR spectra of PMMA are shown
21
22 202 in **Fig. 3a** (Wootthikanokhan et al., 1996). The methyl protons of PMMA (at b region) were
23
24 203 observed at chemical shifts around of $\delta 1.022$ and $\delta 0.846$, whereas protons at c region, the
25
26 204 higher chemical shifts at $\delta 3.645$ and $\delta 3.597$ were found because of the presence of the oxygen
27
28 205 atom attached to its neighboring carbon atom (Fujii et al., 2020). The two peaks at c region
29
30 206 represented the isotactic PMMA structure (Rachellowe, 2017). Moreover, the δ values of
31
32 207 protons attached to the carbon atom in the main chain ($-\text{CH}_2-$) appeared at 1.732 ppm (at a
33
34 208 region). In the case of the AR, the protons which attached to oxygen atom (at f and g region)
35
36 209 appeared at $\delta 4.117$ and $\delta 1.249$, respectively (Kader & Bhowmick, 2000). A proton opposite
37
38 210 with ethyloxy group was appeared at $\delta 2.291$. However, the δ values of proton attached to the
39
40 211 carbon atom in the main chain ($-\text{CH}_2$) appeared at 1.548 ppm (at d region), as shown in
41
42 212 **Fig. 3b** (Kader & Bhowmick, 2000). Considering the ^1H -NMR spectrum of 50AR/PMMA
43
44 213 blend (**Fig. 3c**), the δ values of proton attached to the carbon atom in the main chain shifted
45
46 214 from 1.732 ppm to 1.642 ppm for PMMA, while shifted from 1.548 ppm to 1.621 ppm for AR.
47
48 215 According to the literature (Green, 1974; Kader & Bhowmick, 2000; Soman & Kelkar, 2009),
49
50 216 the change of FTIR and NMR spectra of AR, PMMA, and 50AR/PMMA blend could indicate
51
52 217 the interaction between PMMA and AR phase. **Fig. 4** shows the possible interactions between
53
54
55
56
57
58
59
60

AR and PMMA phases. The dipole-dipole interaction between carbonyl group of PMMA and AR could form in 50AR/PMMA blend.

The addition of TiO_2 in the AR/PMMA blend could disturb the interaction between AR and PMMA phases. The possible mechanism shows in **Fig. 5a**, the hydroxyl group on the TiO_2 could react with the carbonyl group of the AR phase. This claim was in good agreement with the findings of Liu et al. (2003). They claimed that TiO_2 could interfere with the interaction of poly(ethylene oxide) (PEO) and lithium tetrafluoroborate (LiBF_4) by the formation the hydrogen bonding between ether atom of PEO and a hydroxyl group of TiO_2 . Moreover, the non-treated TiO_2 could form the agglomeration structure and act as stress concentration, caused the interference of impact force transfer (Elsaka et al., 2011; Tangudom et al., 2018; Tanumiharja et al., 2000). According to our previous (Tangudom et al., 2019), the stress concentration was diminished by the uniform distribution of TiO_2 particles in the blend with high AR content, resulting in the slight increase in the tensile strength with the addition of 30 to 50 wt% of AR contents. Considering the tensile strength of the $\text{AR}^{\text{t-TiO}_2}$ /PMMA blend, it was higher than that of the AR^{TiO_2} /PMMA blend. Because the KBM603 molecules could diminish the hydrophilic properties on the TiO_2 surface (Huang et al., 2010; Xiao et al., 2017) and form the chemical bonding with the AR phase, as shown in **Fig. 5b**. The silanol group of KBM603 could interact with the hydroxyl group on non-treated TiO_2 particle and the amino group could interact with the chlorine reactive site of the AR chain, resulting in the increase of tensile strength. Many studies have claimed that the rubber-filler interaction was enhanced by the appropriate silane coupling agent (Bansod et al., 2015; Kapgate et al., 2014; Scotti et al., 2012; Wahba et al., 2013).

Fig. 1b and **1c** show the percentage of elongation at break and tensile toughness of AR/PMMA and AR/PMMA blend with non-treated and treated TiO_2 , respectively. Similar to

the tensile strength in **Fig. 1a**, the elongation at break and tensile toughness of AR^{TiO₂}/PMMA blend were lower than those of the AR/PMMA blend only at 10 and 20 wt% of AR content. Because the dipole-dipole interaction of AR/PMMA blend was interfered by the non-treated TiO₂. Moreover, the non-treated TiO₂ could form the agglomeration structure and act as stress concentration during the tensile test (Elsaka et al., 2011; Tanumiharja et al., 2000). However, this interference was diminished in the blend with high AR contents (30-50 wt%), as mentioned earlier. The elongation at break and tensile toughness of the AR^{t-TiO₂}/PMMA blend was higher than that of the AR^{TiO₂}/PMMA blend. It was associated with the influence of the chemical interaction in AR/PMMA blend by KBM603 molecule. AR and PMMA phase was compatible by the polar interaction. Meanwhile, the macromolecule of the AR/PMMA phase was connected by the treated TiO₂. In other words, the treated TiO₂ could form the chemical bonding in the AR/PMMA blend, which was stronger than that of the polar bonding. This is probably why the elongation at break and tensile toughness of the AR^{t-TiO₂}/PMMA blend was higher than that of the AR^{TiO₂}/PMMA blend. Moreover, the KBM603 decreased the agglomeration of TiO₂ particle, resulting in decreasing of the stress concentration in AR/PMMA blend (Carballeira & Hauptert, 2009).

Fig. 6a shows the tensile strength of AR/PMMA and AR/PMMA with non-treated and treated HPQM. It was observed that the tensile strength of the AR^{HPQM}/PMMA blend with 10 and 20 wt% of AR contents was lower than that of the AR/PMMA blend. Considering the chemical structure of the non-treated HPQM molecule, it has a amino group in the structure (Eksirinimitr et al., 2016) as shown in **Fig. 7a**. The amino group could interact with the carbonyl groups of the AR molecule via hydrogen bonding, which interfered the compatibility between AR and PMMA phases. It would be noticed that the tensile strength of AR^{HPQM}/PMMA blend with 30 to 50 wt% of AR content was higher than that of the AR/PMMA blend, this being associated with the influence of the crosslink structure in AR phase by the

reaction between HPQM solution and AR molecules (Tangudom et al., 2019). Regarding the effect of treated HPQM, the tensile strength of AR^{t-HPQM}/PMMA blend was higher than that of the AR^{HPQM}/PMMA blend. Because the silanol group of the KBM603 molecule could interact with the carboxylic salt of non-treated HPQM molecule (Habekost et al., 2013), as shown in **Fig. 7b**. Moreover, the amino group of KBM603 could interact with the chlorine reactive site of AR chain, as expected, caused the enhancement of tensile strength. The percentage of elongation at break and tensile toughness of AR/PMMA and AR/PMMA blend with non-treated and treated HPQM shown in **Fig. 6b** and **6c**, respectively. This suggests that the elongation at break and tensile toughness of AR^{HPQM}/PMMA blend with 10 and 20 wt% of AR content were lower than those of the AR/PMMA blend due to the interference of HPQM molecules. According to our previous work (Tangudom et al., 2019), this interference was diminished by the crosslink structure in AR phase by the reaction between HPQM and AR molecules. Moreover, the addition of treated HPQM in AR/PMMA blend enhanced the elongation at break and tensile toughness, due to the chemical interaction in AR/PMMA blend by KBM603 molecule, as discussed earlier. Thus, it could be claimed that the KBM603 molecule acts as the silane coupling agent for TiO₂ particle and HPQM molecules and the crosslinker for AR/PMMA blend.

However, it was noticeable that the AR/PMMA blend with 10 and 20 wt% of AR content with non-treated and treated TiO₂ and HPQM shows the high tensile strength, but the elongation at break and tensile toughness was low. Meanwhile, the tensile strength of AR/PMMA blend with 30 to 50 wt% of AR content was low, but the elongation at break and tensile toughness were high. The explanation of these results would be related to phase reversion, which affected the properties of the AR/PMMA blend. The morphology of AR/PMMA blend with low AR content was the AR dispersed in PMMA matrix phase (Tangudom et al., 2018). Therefore, the properties of the AR/PMMA blend were controlled by

the PMMA phase (high tensile strength, low elongation at break, and tensile toughness). However, the AR/PMMA blend with high AR content (30 to 50 wt% of AR content) in AR/PMMA blend changed the morphology to the co-continuous phase between AR and PMMA. If so, it can be postulated that the properties of AR/PMMA blend with high AR content were controlled by the AR phase. In other words, they were a rubber-like material, resulting in the low tensile strength and the high elongation at break and tensile toughness. Our results corresponded very well to the findings of Amoabeng et al. (Amoabeng et al., 2017) observed the morphology of polyisobutylene (PIB) and polyethylene oxide (PEO) blend. They found that the co-continuous phase of the PEO/PIB blend has occurred when adding equal or higher than 30 wt% of PEO content. Moreover, the decreasing of the tensile properties of AR^{TiO₂}/PMMA and AR^{HPQM}/PMMA blend as compared with AR/PMMA blend did not pronounce with 30 to 50 wt% of AR content. The explanation for the AR^{TiO₂}/PMMA blend relates to the uniform force transfer. According to our previous work (Tangudom et al., 2018), the distribution of TiO₂ particle in AR/PMMA blend at high AR content was more uniform than that of the low content, which could regularly distribute force during the tensile test. In the case of the AR^{HPQM}/PMMA blend, this would probably be caused by the chemical interaction of the HPQM and AR phase. The amino group of HPQM molecule could interact with the chlorine reactive site of AR phase and form the chemical interaction and form the chemical interaction with the AR phase, resulting in the increase of tensile properties (Tangudom et al., 2019).

Fig. 8a and 8b show the impact strength of AR/PMMA and AR/PMMA blends with non-treated and treated of TiO₂ and HPQM, respectively. The impact strength depends on the energy consumption for damage PMMA and AR phase (Collyer, 1994; Thankappan Nair et al., 2015), which differs from the tensile toughness. It was seen that the impact strength of AR^{TiO₂}/PMMA was lower than that of the AR/PMMA blend. Because non-treated TiO₂ particle

did not compatible with the AR phase, caused the interference of the impact force transfer (Tangudom et al., 2018). For the impact strength of the AR^{TiO₂}/PMMA blend, it was higher than that of the AR^{TiO₂}/PMMA. It could be associated with the crosslinked structure in the AR phase from treated-TiO₂ could adsorb the impact force during the test. In the case of AR^{HPQM}/PMMA, the impact strength tended to be higher than that of AR/PMMA. According to the earlier discussion, the amino group of the HPQM molecule could form the crosslinked structure by the interaction with the chlorine reactive site group of the AR phase. If so, it can be postulated that the impact force was adsorbed by their crosslink structure. However, the impact strength of the AR^{t-HPQM}/PMMA blend tends to be higher than that of the AR^{HPQM}/PMMA blend. According to the scheme, as shown in **Fig. 7b**, the KBM603 molecule could interact with chlorine reactive site of AR phase and form the crosslinked structure, which adsorbed the impact force (Asaletha et al., 1999; Hesami & Jalali-Arani, 2018; Jiang et al., 2014; Lee & Han, 1999). The evidence, which investigated the interference of TiO₂ and HPQM, was the FTIR spectrum at the carbonyl group position. **Fig. 9** shows the FTIR spectrum of the 50AR/PMMA, 50AR^{TiO₂}/PMMA, and 50AR^{HPQM}/PMMA. The results show that the FTIR spectrums of the carbonyl group of the 50AR/PMMA phase shift from 1723 cm⁻¹ to 1725 cm⁻¹ of the 50AR^{TiO₂}/PMMA, and AR^{HPQM}/PMMA, which supported the occurrence of the weak interaction between AR phase and the antibacterial agents (TiO₂ and HPQM). It could be concluded that the interference of the antibacterial agent decreased the compatibility between PMMA and AR phases, and this resulted in the discontinuous force transfer during the impact test.

Antibacterial performance of AR/PMMA blends filled with non-treated and treated TiO₂ and HPQM

The quantitative antibacterial activities using R value of AR/PMMA blend with non-treated and treated TiO_2 and HPQM against the growth of *E. coli* using JIS Z2801 specifications are given in **Fig. 10**. If the R value is equal to or higher than 2.0, bacterial reduction approaches 99.9%, and the sample is accepted as an antibacterial material (Association, 2010). It was seen that the AR^{TiO_2} /PMMA blend did not act as the antibacterial material. However, the R-value of the $\text{AR}^{\text{t-TiO}_2}$ /PMMA blend was higher than 2.0, as shown in **Fig. 10a**. Because the chemical reaction of the AR phase and treated TiO_2 particle established the large free volume between the AR-PMMA molecule, which increased the flexibility in AR/PMMA blend. Work by Gali et al. (2016) claimed that TiO_2 could generate O_2^- , HOO^\bullet , and HO^\bullet in the dark due to dissolved oxygen. Thus, it can be speculated that the oxygen from the environment and bacterial suspension could support the ROS generation from TiO_2 . Therefore, the ROS could move to contact with bacteria cell by the free volume of the AR/PMMA blend. However, the R value of $\text{AR}^{\text{t-TiO}_2}$ /PMMA blend at 40 and 50 wt% of AR content slightly decreased. The assumption of this result, the TiO_2 particles were embedded under the sample surface. Considering the morphology of AR/PMMA blend with low AR contents, 10 to 30 wt% in this case, the AR was a dispersed phase in PMMA matrix (Tangudom et al., 2018). The treated TiO_2 particles in the AR dispersed phase could interact with dissolve oxygen and generate ROS to inhibit bacteria cell growth. Meanwhile, the co-continuous morphology demonstrated for the AR/PMMA blend with high AR contents (40 and 50 wt%). Some of treated TiO_2 particles were embedded underneath the sample, which reduced the interaction between TiO_2 particles and dissolve oxygen. Therefore, the inhibition of bacteria cell growth by ROS decreased. Nevertheless, it was noted that the R value of $\text{AR}^{\text{t-TiO}_2}$ /PMMA blend after exposure to UV radiation was higher than 2.0 and was higher than that of the AR^{TiO_2} /PMMA. Because the excess ROS was increased by the photocatalysis process from TiO_2 particle.

Fig. 10b shows the antibacterial activities of AR/PMMA blend with non-treated and treated HPQM against the growth of *E. coli*. It was observed that the R value of AR^{HPQM}/PMMA and AR^{t-HPQM}/PMMA blend was higher than 2.0. HPQM molecules are the organic material which solutes in the water, and they could penetrate throughout the specimen to contact with bacteria cell wall by the stress concentration gradian theory (Eksirinimitr et al., 2016; Tangudom et al., 2019). In the case of the effect of UV radiation, the R value of AR^{t-HPQM}/PMMA blend was still higher than 2.0. Because the HPQM and KBM603 molecule could form the weak polar interaction. After exposure to UV radiation, the polar interaction of treated HPQM was destroyed, which supported the generation of HPQM molecule throughout the specimen. It could be concluded that KBM603 recommended for treated in the TiO₂ and HPQM to improve the mechanical properties for all AR/PMMA content. Considering the antibacterial performance of AR/PMMA blend, the treated TiO₂ and HPQM by KBM603 recommended for the hygiene products which were exposed to UV radiation.

Conclusions

The addition of non-treated of TiO₂ and HPQM decreased the mechanical properties of AR/PMMA blend, whereas the treated of TiO₂ and HPQM by KBM603 in AR/PMMA blend increased. The treatment of TiO₂ and HPQM increased the free volume and flexibility in AR/PMMA blend due to the chemical reaction. The evidence provided by FTIR and ¹H-NMR. Considering the antibacterial performance, the AR/PMMA blend with non-treated and treated HPQM could act as the antibacterial material. Therefore, the AR^{t-HPQM}/PMMA blend with 10 and 20 wt% of AR content was recommended for the sanitarywares, which demand the high tensile strength and toughness, such as the shower cabin. Meanwhile, the AR^{t-HPQM}/PMMA blend with 30 to 50 wt% of AR content was recommended for the cover sheet of the shower bath, which need the high elongation during the processing. Meanwhile, the AR^{TiO2}/PMMA

1
2
3
4
5
6
7
8
9
10
11
12
13
14
15
16
17
18
19
20
21
22
23
24
25
26
27
28
29
30
31
32
33
34
35
36
37
38
39
40
41
42
43
44
45
46
47
48
49
50
51
52
53
54
55
56
57
58
59
60

blend did not show the antibacterial performance, but the AR^{t-TiO₂}/PMMA blend could inhibit bacterial cell growth with 10 to 30 wt% of AR content. Therefore, the AR^{t-TiO₂}/PMMA blend with 10 to 30 wt% of AR content was recommended for the sanitarywares, which demand the high tensile strength and toughness. Moreover, the treated TiO₂ and HPQM by KBM603 recommended for the hygiene products which were exposed to UV radiation for all AR/PMMA content.

Conflict of interest

The authors declare no conflict of interest.

Acknowledgements

The authors would like to thank the Office of the Higher Education Commission (OHEC) under the National Research University (NRU) Program and the Thailand Research Fund (TRF) under the Royal Golden Jubilee Ph.D. Program (PHD/0151/2557). The authors are grateful to the College of Industrial Technology, King Mongkut’s University of Technology North Bangkok (KMUTNB), the Faculty of Environment and Resource Studies, Mahidol University, and the Department of Materials, Loughborough University for supplying laboratory facilities.

References

- Alrahlah, A., Fouad, H., Hashem, M., Niazy, A. A., & AlBadah, A. (2018). Titanium Oxide (TiO₂)/Polymethylmethacrylate (PMMA) Denture Base Nanocomposites: Mechanical, Viscoelastic and Antibacterial Behavior. *Materials (Basel)*, 11(7), 1-15. <http://doi.org/10.3390/ma11071096>
- Ambrósio, J. D., Balarim, C. V. M., & De-Carvalho, G. B. (2016). Preparation, Characterization, and Mechanical/Tribological Properties of Polyamide 11/Titanium Dioxide Nanocomposites. *Polymer Composites*, 37(5), 1415-1424. <http://doi.org/10.1002/pc.23310>
- Amoabeng, D., Roell, D., Clouse, K. M., Young, B. A., & Velankar, S. S. (2017). A Composition-Morphology Map for Particle-Filled Blends of Immiscible Thermoplastic Polymers. *Polymer*, 119, 212-223. <https://doi.org/10.1016/j.polymer.2017.04.009>
- An, J., Kang, B. H., Choi, B. H., & Kim, H. J. (2014). Observation and Evaluation of Scratch Characteristics of Injection-Molded Poly(methyl methacrylate) Toughened by Acrylic Rubbers. *Tribology International*, 77(1), 32-42. <http://doi.org/10.1016/j.triboint.2014.04.011>
- Asaletha, R., Kumarana, M. G., & Thoma, S. (1999). Thermoplastic Elastomers from Blends of Polystyrene and Natural Rubber Morphology and Mechanical Properties. *European Polymer Journal*, 35, 253-271. [https://doi.org/10.1016/S0014-3057\(98\)00115-3](https://doi.org/10.1016/S0014-3057(98)00115-3)
- Association, J. S. (2010). JIS Z2801 Antibacterial products In *Test for antibacterial activity and efficacy* (pp. 27). Japan: Japanese Standards Association.

- 427 Bansod, N. D., Kapgate, B. P., Das, C., Basu, D., Debnath, S. C., Roy, K., & Wiessner, S.
428 (2015). Controlled Growth of In Situ Silica in a NR/CR Blend by a Solution Sol–Gel
429 Method and the Studies of Its Composite Properties. *RSC Advances*, 5(66), 53559-
430 53568. <http://doi.org.10.1039/c5ra08971a>
- 431 Carballeira, P., & Hauptert, F. (2009). Toughening Effects of Titanium Dioxide Nanoparticles
432 on TiO₂/Epoxy Resin Nanocomposites. *Polymer Composites*(1), 1241-1246.
433 <http://doi.org.10.1002/pc.20911>
- 434 Chung, C. J., Lin, H. I., & He, J. L. (2007). Antimicrobial Efficacy of Photocatalytic TiO₂
435 Coatings Prepared by Arc Ion Plating. *Surface and Coatings Technology*, 202(4-7),
436 1302-1307. <http://doi.org.10.1016/j.surfcoat.2007.07.077>
- 437 Cocco, D. R., De Carvalho, F. P., & Felisberti, M. I. (2013). Structures and Morphologies
438 Olefin Situ-polymerized Blends of PMMA and ASA. *Journal of Applied Polymer
439 Science*, 130(1), 654-664. <http://doi.org.10.1002/app.39188>
- 440 Collyer, A. A. (1994). *Rubber Toughened Engineering Plastics*. Springer Science+Business
441 Media Dordrecht
- 442 Duan, G., Zhang, C., Li, A., Yang, X., Lu, L., & Wang, X. (2008). Preparation and
443 Characterization of Mesoporous Zirconia Made by Using a Poly (methyl methacrylate)
444 Template. *Nanoscale Res Lett*, 3(3), 118-122. [http://doi.org.10.1007/s11671-008-9123-
445 7](http://doi.org.10.1007/s11671-008-9123-7)
- 446 Eksirinimitr, A., Wimolmala, E., Taptim, K., & Sombatsompop, N. (2016). Effects of
447 Simulation Conditions on Antibacterial Performance of Polypropylene and Polystyrene
448 Doped with HPQM Antibacterial Agent. *Polymer Testing*, 55(1), 123-134.
449 <http://doi.org.10.1016/j.polymertesting.2016.08.012>

- 450 Elsaka, S. E., Hamouda, I. M., & Swain, M. V. (2011). Titanium Dioxide Nanoparticles
451 Addition to a Conventional Glass-Ionomer Restorative: Influence on Physical and
452 Antibacterial Properties. *Journal of Dentistry*, 39(9), 589-598. [http://doi.org.10.1016/](http://doi.org.10.1016/j.jdent.2011.05.006)
453 [j.jdent.2011.05.006](http://doi.org.10.1016/j.jdent.2011.05.006)
- 454 Fujii, N., Miyauchi, T., Oda, T., Bhowmick, A. K., & Saha, T. (2020). Influence of
455 Fluoroacrylate Cure Site Monomer on the Thermal and Mechanical Properties of the
456 Polyacrylic Ester Elastomer. *Rubber Chemistry and Technology*, 93(2), 395-413.
457 <http://doi.org.10.5254/rct.19.80440>
- 458 Gali, N. K., Ning, Z., Daoud, W., & Brimblecombe, P. (2016). Investigation on the Mechanism
459 of Non-Photocatalytically TiO₂-Induced Reactive Oxygen Species and Its Significance
460 on Cell Cycle and Morphology. *Journal of Applied Toxicology*, 36(10), 1355-1363.
461 <http://doi.org.10.1002/jat.3341>
- 462 Green, R. D. (1974). The Nature of C—H Hydrogen Bonding. In R. D. Green (Ed.), *Hydrogen*
463 *Bonding by C—H Groups* (pp. 158-167). Wiley.
- 464 Habekost, L. V., Camacho, G. B., Lima, G. S., Ogliari, F. A., Piva, E., & Moraes, R. R. (2013).
465 Properties of Particulate Resin-Luting Agents with Phosphate and Carboxylic
466 Functional Methacrylates as Coupling Agents. *Journal of Applied Polymer Science*,
467 127(5), 3467-3473. <http://doi.org.10.1002/app.37627>
- 468 Haddadi, E., Choupani, N., & Abbasi, F. (2016). Experimental investigation on the mixed-
469 mode fracture of rubber-toughened PMMA using essential work of fracture method.
470 *Engineering Fracture Mechanics*, 162, 112-120. [http://doi.org.10.1016/j.engfracmech.](http://doi.org.10.1016/j.engfracmech.2016.05.011)
471 2016.05.011

- 472 Hesami, M., & Jalali-Arani, A. (2018). Morphology Development Via Static Crosslinking of
473 (Polylactic acid/Acrylic rubber) as an Immiscible Polymer Blend. *Macromolecular*
474 *Materials and Engineering*, 303(3), 1700446. <http://doi.org.10.1002/mame.201700446>
- 475 Huang, L., Chen, K., Lin, C., Yang, R., & Gerhardt, R. A. (2010). Fabrication and
476 Characterization of Superhydrophobic High Opacity Paper with Titanium Dioxide
477 Nanoparticles. *Journal of Materials Science*, 46(8), 2600-2605. <http://doi.org.10.1007/s10853-010-5112-1>
- 479 Jiang, X., Xu, C., Wang, Y., & Chen, Y. (2014). Polyvinylidene Fluoride/Acrylonitrile
480 Butadiene Rubber Blends Prepared Via Dynamic Vulcanization. *Journal of*
481 *Macromolecular Science Part B Physics*, 54(1), 58-70. [http://doi.org.10.1080/0022](http://doi.org.10.1080/00222348.2014.984577)
482 [2348.2014.984577](http://doi.org.10.1080/00222348.2014.984577)
- 483 Kader, M. A., & Bhowmick, A. K. (2000). New Miscible Elastomer Blend from Acrylate
484 Rubber. *Rubber Chemistry and Technology*, 73(5), 889-901. [http://doi.org.10.5254/](http://doi.org.10.5254/1.3547627)
485 [1.3547627](http://doi.org.10.5254/1.3547627)
- 486 Kapgate, B. P., Das, C., Basu, D., Das, A., Heinrich, G., & Reuter, U. (2014). Effect of Silane
487 Integrated Sol-Gel Derived in Situ Silica on the Properties of Nitrile Rubber. *Journal*
488 *of Applied Polymer Science*, 131(15), 40054. <http://doi.org.10.1002/app.40531>
- 489 Lee, B. H., Chang, Y. W., & Lim, H. M. (2015). Preparation and Characterizations of
490 Polymethylmethacrylate (PMMA)/Acrylate Rubber (ACM) Blend for Light Diffuser
491 Applications. *Elastomers and Composites*, 50(1), 49-54. [http://doi.org.10.7473/ec.](http://doi.org.10.7473/ec.2015.50.1.049)
492 [2015.50.1.049](http://doi.org.10.7473/ec.2015.50.1.049)
- 493 Lee, J. K., & Han, C. D. (1999). Evolution of Polymer Blend Morphology During
494 Compounding in an Internal Mixer. *Polymer*, 40, 6277-6296. [https://doi.org/10.1016/](https://doi.org/10.1016/S0032-3861(99)00022-1)
495 [S0032-3861\(99\)00022-1](https://doi.org/10.1016/S0032-3861(99)00022-1)

- 496 Liu, Y., Lee, J. Y., & Hong, L. (2003). Morphology, Crystallinity, and Electrochemical
497 Properties of In Situ Formed Poly(ethylene oxide) /TiO₂ Nanocomposite Polymer
498 Electrolytes. *Journal of Applied Polymer Science*, 89(1), 2815–2822. <https://doi.org/10.1002/app.12487>
- 500 Lommerse, J. P. M., Pricce, S. L., & Taylor, R. (1998). Hydrogen Bonding of Carbonyl,
501 Ether, and Ester Oxygen Atoms with Alkanol Hydroxyl Groups. *Journal of*
502 *Computational Chemistry*, 18(6), 757-774. [https://doi.org/10.1002/\(SICI\)1096-](https://doi.org/10.1002/(SICI)1096-987X(19970430)18:6<757::AID-JCC3>3.0.CO;2-R)
503 [987X\(19970430\)18:6<757::AID-JCC3>3.0.CO;2-R](https://doi.org/10.1002/(SICI)1096-987X(19970430)18:6<757::AID-JCC3>3.0.CO;2-R)
- 504 Microsciencetech. (2000, May 29). *Technical data sheet : BCA101A0*. Retrieved from Korea:
505 www.mst21.com
- 506 Nakason, C., Panklieng, Y., & Kaesaman, A. (2004). Rheological and Thermal Properties of
507 Thermoplastic Naturak Rubbers Based on PMMA/EPDM Blends. *Journal of Applied*
508 *Polymer Science*, 92(6), 3561–3572 <https://doi.org/10.1002/app.20384>
- 509 Rachellowe. (2017, August 11). *NMR of PMMA – tacticity and its determination through NMR*.
510 Impact Solution. <https://www.impact-solutions.co.uk/nmr-of-pmma/s>
- 511 Ramesh, S., Leen, K. H., Kumutha, K., & Arof, A. K. (2007). FTIR Studies of PVC/PMMA
512 Blend Based Polymer Electrolytes. *Spectrochimica Acta. Part A: Molecular and*
513 *Biomolecular Spectroscopy*, 66(4-5), 1237-1242. [http://doi.org.10.1016/j.saa.](http://doi.org.10.1016/j.saa.2006.06.012)
514 [2006.06.012](http://doi.org.10.1016/j.saa.2006.06.012)
- 515 Sathya, S., Murthy, P. S., Devi, V. G., Das, A., Anandkumar, B., Sathyaseelan, V. S., Doble,
516 M., & Venugopalan, V. P. (2019). Antibacterial and Cytotoxic Assessment of
517 Poly(methyl methacrylate) Based Hybrid Nanocomposites. *Materials Science and*
518 *Engineering. C: Materials for Biological Applications*, 100, 886-896.
519 <https://doi.org/10.1016/j.msec.2019.03.053>

- 520 Scotti, R., Wahba, L., Crippa, M., D'Arienzo, M., Donetti, R., Santo, N., & Morazzoni, F.
521 (2012). Rubber–Silica Nanocomposites Obtained by In Situ Sol–Gel Method: Particle
522 Shape Influence on the Filler–Filler and Filler–Rubber Interactions. *Soft Matter*, 8(7),
523 2131-2143. <http://doi.org.10.1039/c1sm06716h>
- 524 Shen, S. C., Letchmanan, K., Chow, P. S., & Tan, R. B. H. (2019). Antibiotic Elution and
525 Mechanical Property of TiO₂ Nanotubes Functionalized PMMA-based Bone Cements.
526 *Journal of the Mechanical Behavior of Biomedical Materials*, 91, 91-98.
527 <https://doi.org/10.1016/j.jmbbm.2018.11.020>
- 528 Sodagar, A., Khalil, S., Kassae, M. Z., Shahroudi, A. S., Pourakbari, B., & Bahador, A.
529 (2016). Antimicrobial Properties of Poly (methyl methacrylate) Acrylic Resins
530 Incorporated with Silicon Dioxide and Titanium Dioxide Nanoparticles on Cariogenic
531 Bacteria. *Journal of orthodontic science*, 5(1), 7-13. [http://doi.org.10.4103/2278-](http://doi.org.10.4103/2278-0203.176652)
532 [0203.176652](http://doi.org.10.4103/2278-0203.176652)
- 533 Soman, V. V., & Kelkar, D. S. (2009). FTIR Studies of Doped PMMA - PVC Blend System.
534 *Macromolecular Symposia*, 277(1), 152-161. <http://doi.org.10.1002/masy.200950319>
- 535 Sombatsompop, N., & Chaochanchaikul, K. (2005). Average Mixing Torque, Tensile and
536 Impact Properties, and Thermal Stability of Poly(vinyl chloride)/Sawdust Composites
537 with Different Silane Coupling Agents. *Journal of Applied Polymer Science*, 96(1),
538 213-221. <http://doi.org.10.1002/app.21422>
- 539 Tan, H., Peng, Z., Li, Q., Xu, X., Guo, S., & Tang, T. (2012). The use of Quaternised Chitosan-
540 loaded PMMA to Inhibit Biofilm Formation and Downregulate the Virulence-
541 associated Gene Expression of Antibiotic-resistant *Staphylococcus*. *Biomaterials*,
542 33(2), 365-377. <https://doi.org/10.1016/j.biomaterials.2011.09.084>

- 543 Tangboriboon, N., Sirivat, A., Kunanurksapong, R., & Wongkasemjit, S. (2009).
544 Electrorheological Properties of Novel Piezoelectric Lead Zirconate Titanate
545 $\text{Pb}(\text{Zr}_{0.5}\text{Ti}_{0.5})\text{O}_3$ -acrylic Rubber Composite. *Materials Science and Engineering: C*,
546 29(6), 1913-1918. <http://doi.org.10.1016/j.msec.2009.03.002>
- 547 Tangboriboon, N., Sirivat, A., & Wongkasemjit, S. (2008). Electrorheology and
548 Characterization of Acrylic Rubber and Lead Titanate Composite Materials. *Applied*
549 *Organometallic Chemistry*, 22(5), 262-269. <http://doi.org.10.1002/aoc.1388>
- 550 Tangudom, P., Wimolmala, E., Prapagdee, B., & Sombatsompop, N. (2018). Material
551 Formulations for AR/PMMA and AR- TiO_2 /PMMA Blends and Effects of UV
552 Radiation and TiO_2 Loading on Mechanical and Antibacterial Performances. *Polymer-*
553 *Plastics Technology and Engineering*, 57(18), 1963-1976. [http://doi.org.10.1080/](http://doi.org.10.1080/03602559.2018.1447131)
554 03602559.2018.1447131
- 555 Tangudom, P., Wimolmala, E., Prapagdee, B., & Sombatsompop, N. (2019). Mechanical
556 Properties and Antibacterial Performance of PMMA Toughened with Acrylic Rubber
557 Containing 2-Hydroxypropyl-3-Piperazinyl-Quinoline Carboxylic Acid Methacrylate
558 (HPQM) and HPQM Absorbed on TiO_2 Particles. *Polymer Testing*, 79(1), 106023.
559 <http://doi.org.10.1016/j.polymertesting.2019.106023>
- 560 Tanumiharja, M., Burrow, M. F., & Tyas, M. J. (2000). Microtensile Bond Strengths of Glass
561 Ionomer (Polyalkenoate) Cements to Dentine Using Four Conditioners. *Journal of*
562 *Dentistry for Children*, 28(1), 6. [http://doi.org.10.1016/s0300-5712\(00\)00009-9](http://doi.org.10.1016/s0300-5712(00)00009-9)
- 563 Thankappan Nair, S., Vijayan, P. P., Xavier, P., Bose, S., George, S. C., & Thomas, S. (2015).
564 Selective Localisation of Multi Walled Carbon Nanotubes in Polypropylene/Natural
565 Rubber Blends to Reduce the Percolation Threshold. *Composites Science and*
566 *Technology*, 116(1), 9-17. <https://doi.org/10.1016/j.compscitech.2015.04.021>

- 567 Wahba, L., D'Arienzo, M., Donetti, R., Hanel, T., Scotti, R., Tadiello, L., & Morazzoni, F.
568 (2013). In Situ Sol–Gel Obtained Silica–Rubber Nanocomposites: Influence of the
569 Filler Precursors on the Improvement of the Mechanical Properties. *RSC Advances*,
570 3(17), 5832–5844. <http://doi.org.10.1039/c3ra22706e>
- 571 Wang, J., Zhang, X., Jiang, L., & Qiao, J. (2019). Advances in Toughened Polymer Materials
572 by Structured Rubber Particles. *Progress in Polymer Science*, 98.
573 <http://doi.org.10.1016/j.progpolymsci.2019.101160>
- 574 Wang, L., Jiang, X., Wang, C., Huang, Y., Meng, Y., & Shao, J. (2019). Titanium Dioxide
575 Grafted with Silane Coupling Agents and Its Use in Blue Light Curing Ink. *Coloration*
576 *Technology*, 1(1), 1-8. <http://doi.org.10.1111/cote.12434>
- 577 Wootthikanokhan, J., R, P. B., & Chaplin, R. P. (1996). Effect of Acrylic Diblock Copolymer
578 upon Interfacial Adhesion. *Journal of Applied Polymer Science*, 62, 835-844.
579 [https://doi.org/10.1002/\(SICI\)1097-4628\(19961031\)62:5<835::AID-APP16>3.0.CO;](https://doi.org/10.1002/(SICI)1097-4628(19961031)62:5<835::AID-APP16>3.0.CO;2-R)
580 2-R
- 581 Xiao, Z., Guo, P., & Sun, N. (2017). Preparation, Thermostability, and Hydrophobic Properties
582 of TiO₂/Poly(dodecafluoroheptyl methacrylate) Nanocomposites. *Journal of Applied*
583 *Polymer Science*, 134(2), 44377. <http://doi.org.10.1002/app.44377>
- 584 Zhao, J., Milanova, M., Warmoeskerken, M. M. C. G., & Dutschk, V. (2012). Surface
585 Modification of TiO₂ Nanoparticles with Silane Coupling Agents. *Colloids and*
586 *Surfaces A: Physicochemical and Engineering Aspects*, 413(1), 273-279.
587 <http://doi.org.10.1016/j.colsurfa.2011.11.033>

LIST OF TABLES

Table No.	Table Captions
Table 1	Material formulas.

LIST OF FIGURES

Figure No.	Figure Captions
Figure 1	Tensile properties of AR/PMMA (white) and AR/PMMA blends with non-treated (black) and treated (gray) of TiO ₂ ; tensile strength, (b) percentage of elongation at break, and (c) tensile toughness.
Figure 2	FTIR spectrum of (a) PMMA, (b) AR, and (c) 50AR/PMMA blend.
Figure 3	¹ H-NMR spectrum of (a) PMMA, (b) AR, and (c) 50AR/PMMA blend in deuterated chloroform D (CDCl ₃).
Figure 4	Scheme of the interaction between AR and PMMA phases.
Figure 5	Schematic of the interaction of (a) non-treated and (b) treated TiO ₂ particle in AR/PMMA blend.
Figure 6	Tensile properties of AR/PMMA (white) and AR/PMMA blends with non-treated (black) and treated (pattern) of HPQM; (a) tensile strength, (b) percentage of elongation at break, and (c) tensile toughness.
Figure 7	Schematic of the interaction of (a) non-treated and (b) treated HPQM molecule in AR/PMMA blend.
Figure 8	Impact strength of AR/PMMA (white) and AR/PMMA blends with non-treated (black) and treated (pattern) of (a)TiO ₂ and (b) HPQM.
Figure 9	FTIR spectrum of AR/PMMA, AR ^{TiO2} /PMMA, and AR ^{HPQM} /PMMA in the wavelength range of 1500 to 2000 cm ⁻¹ .
Figure 10	Antibacterial performance of AR/PMMA blends against <i>E. coli</i> with non-treated (black) and treated before (gray) and after (white-dot) exposure to UV radiation; (a) TiO ₂ and (b) HPQM.

1
2
3
4
5
6
7
8
9
10
11
12
13
14
15
16
17
18
19
20
21
22
23
24
25
26
27
28
29
30
31
32
33
34
35
36
37
38
39
40
41
42
43
44
45
46
47
48
49
50
51
52
53
54
55
56
57
58
59
60

7 **Table 1** Material formulas.

Formula	Composition				
	PMMA (wt%)	AR (wt%)	TiO ₂ (pph)	HPQM (pph)	KBM603 (%)
10AR/PMMA	90	10	-	-	-
10AR ^{TiO₂} /PMMA			1.5	-	-
10AR ^{HPQM} /PMMA			-	1.5	-
10AR ^{t-TiO₂} /PMMA			1.5	-	1
10AR ^{t-HPQM} /PMMA			-	1.5	1
20AR/PMMA	80	20	-	-	-
20AR ^{TiO₂} /PMMA			1.5	-	-
20AR ^{HPQM} /PMMA			-	1.5	-
20AR ^{t-TiO₂} /PMMA			1.5	-	1
20AR ^{t-HPQM} /PMMA			-	1.5	1
30AR/PMMA	70	30	-	-	-
30AR ^{TiO₂} /PMMA			1.5	-	-
30AR ^{HPQM} /PMMA			-	1.5	-
30AR ^{t-TiO₂} /PMMA			1.5	-	1
30AR ^{t-HPQM} /PMMA			-	1.5	1
40AR/PMMA	60	40	-	-	-
40AR ^{TiO₂} /PMMA			1.5	-	-
40AR ^{HPQM} /PMMA			-	1.5	-
40AR ^{t-TiO₂} /PMMA			1.5	-	1
40AR ^{t-HPQM} /PMMA			-	1.5	1
50AR/PMMA	50	50	-	-	-
50AR ^{TiO₂} /PMMA			1.5	-	-
50AR ^{HPQM} /PMMA			-	1.5	-
50AR ^{t-TiO₂} /PMMA			1.5	-	1
50AR ^{t-HPQM} /PMMA			-	1.5	1

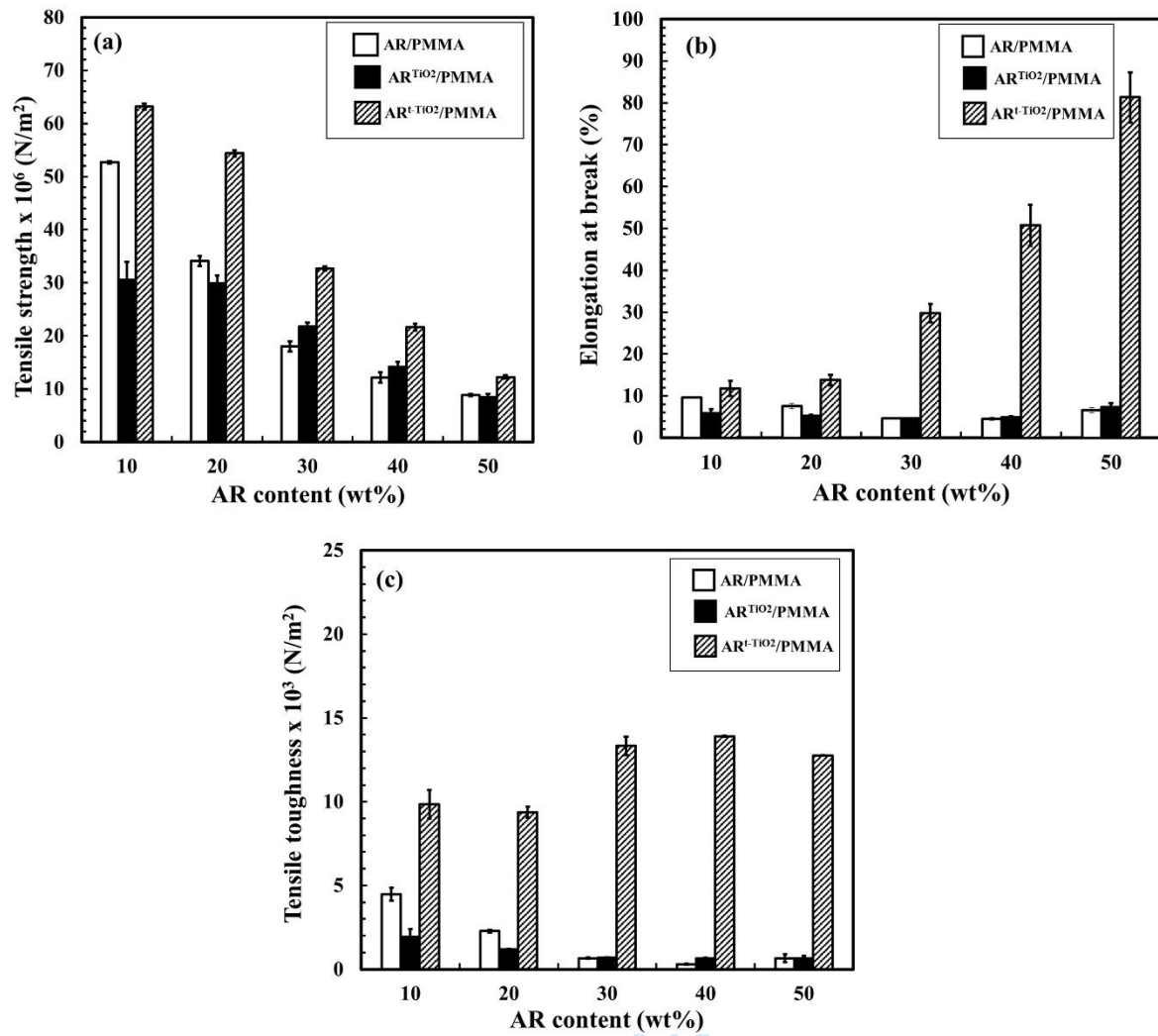


Figure 1 Tensile properties of AR/PMMA (white) and AR/PMMA blends with non-treated (black) and treated (pattern) of TiO₂; (a) tensile strength, (b) percentage of elongation at break, and (c) tensile toughness.

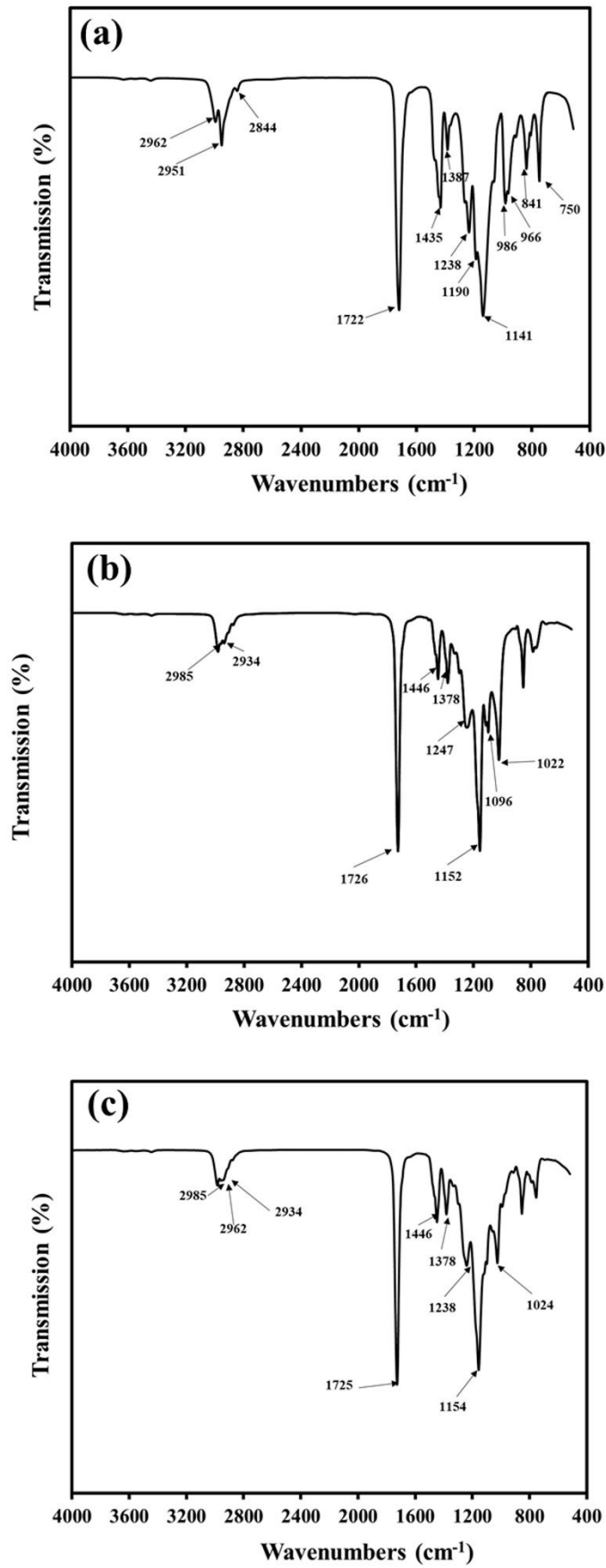


Figure 2 FTIR spectrum of (a) PMMA, (b) AR, and (c) 50AR/PMMA blend.

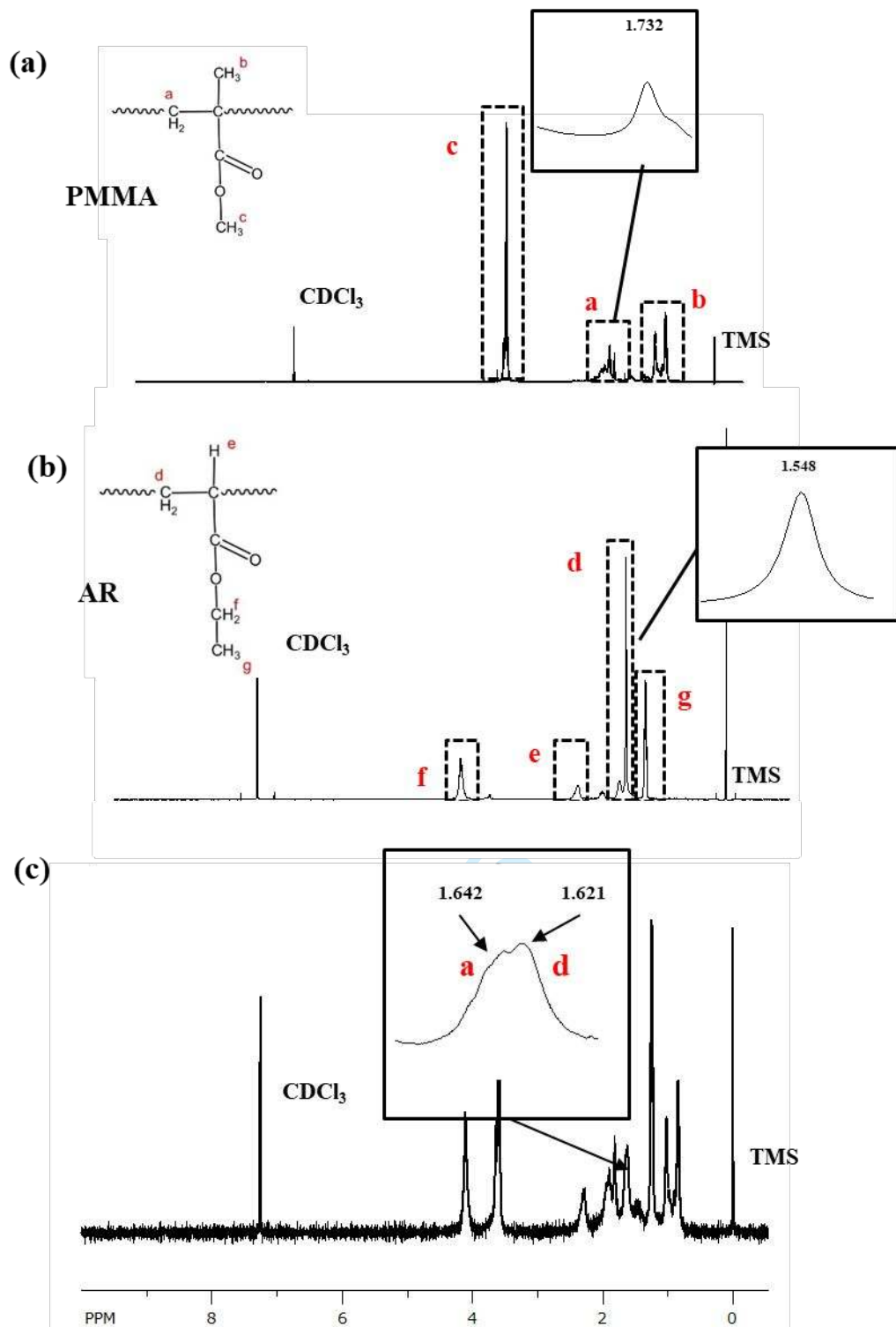


Figure 3 ¹H-NMR spectrum of (a) PMMA, (b) AR, and (c) 50AR/PMMA blend in deuterated chloroform D (CDCl₃).

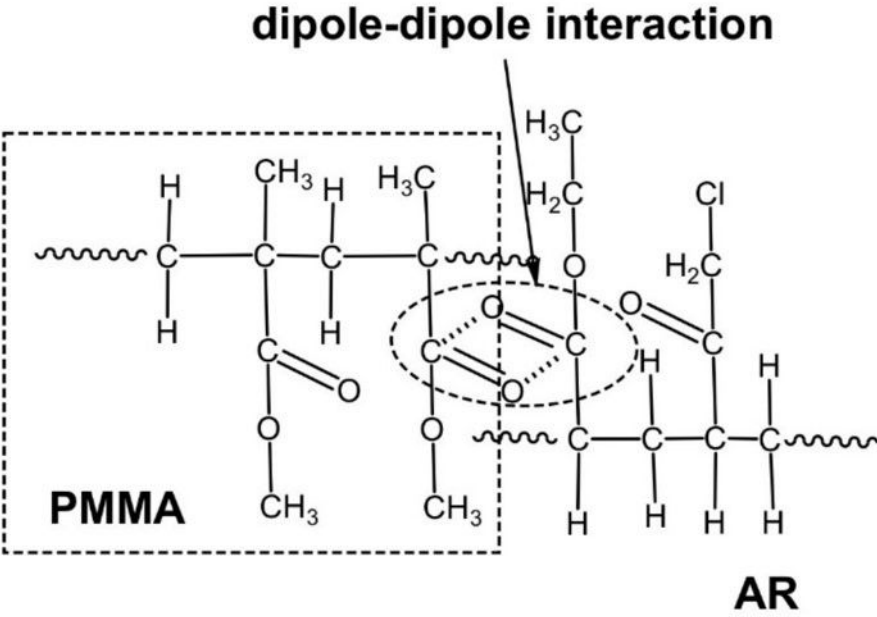
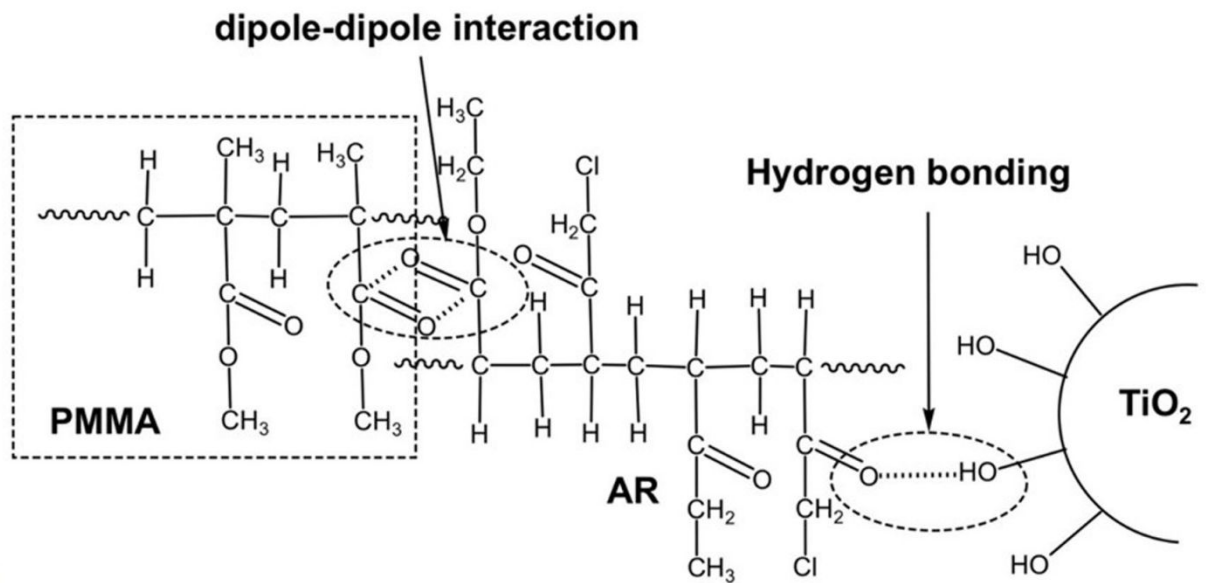


Figure 4 Scheme of the interaction between AR and PMMA phases

(a)



(b)

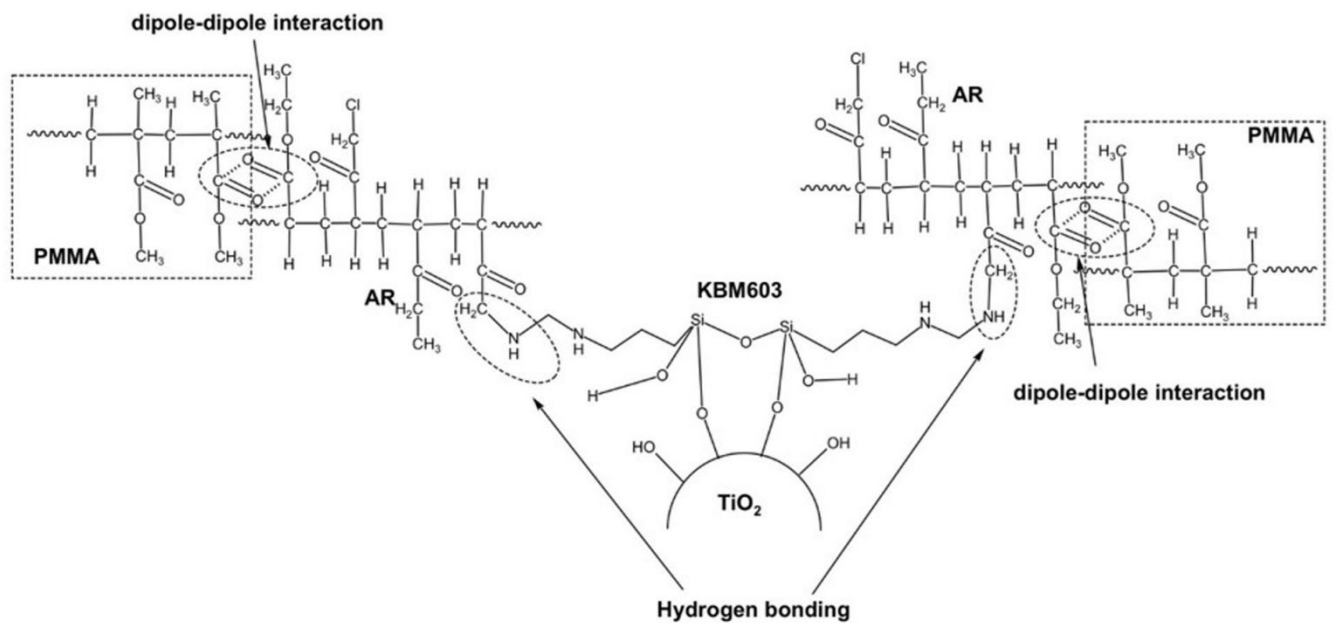


Figure 5 Schematic of the interaction of (a) non-treated and (b) treated TiO₂ particle in AR/PMMA blend.

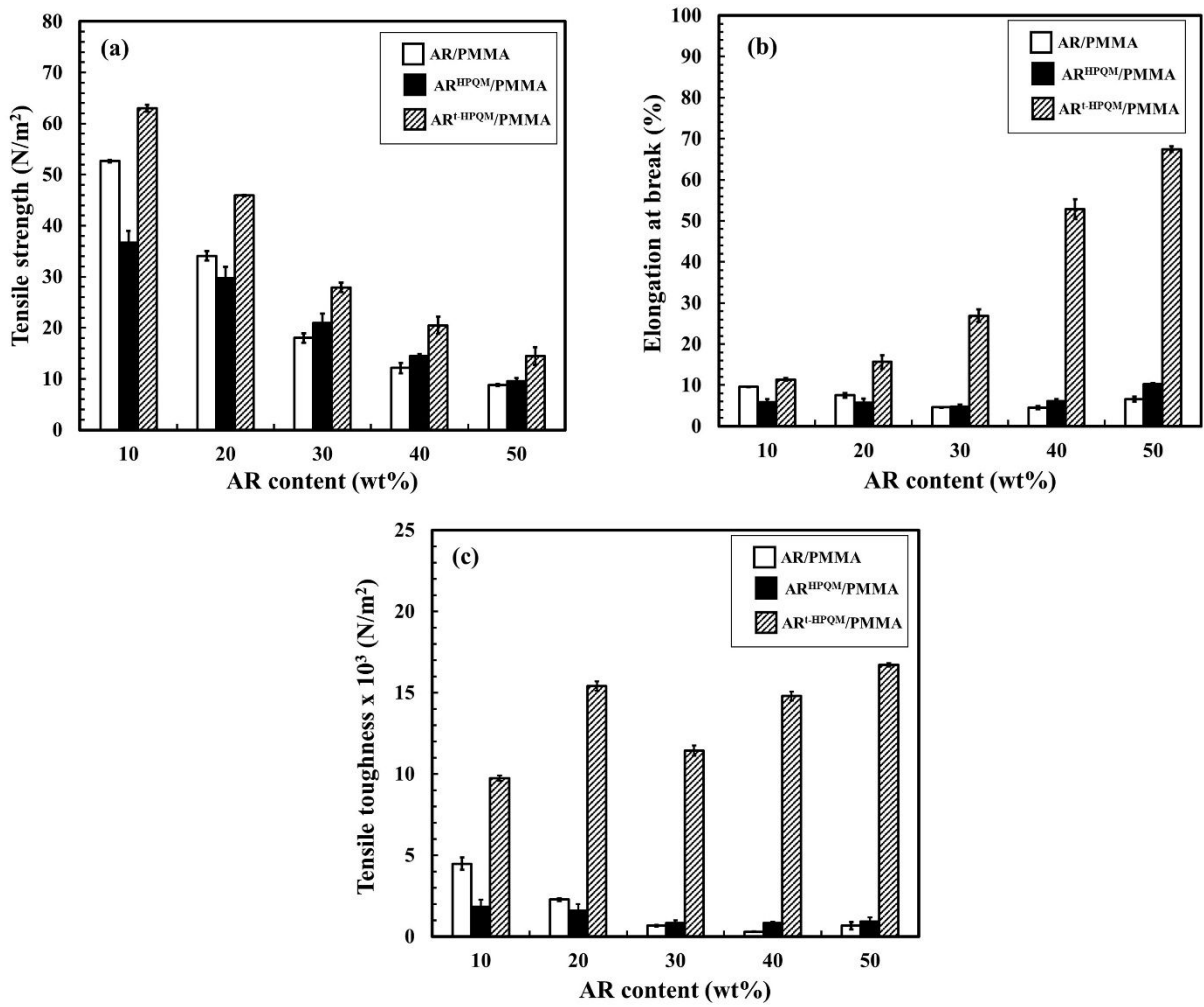


Figure 6 Tensile properties of AR/PMMA (white) and AR/PMMA blends with non-treated (black) and treated (pattern) of HPQM; (a) tensile strength, (b) percentage of elongation at break, and (c) tensile toughness.

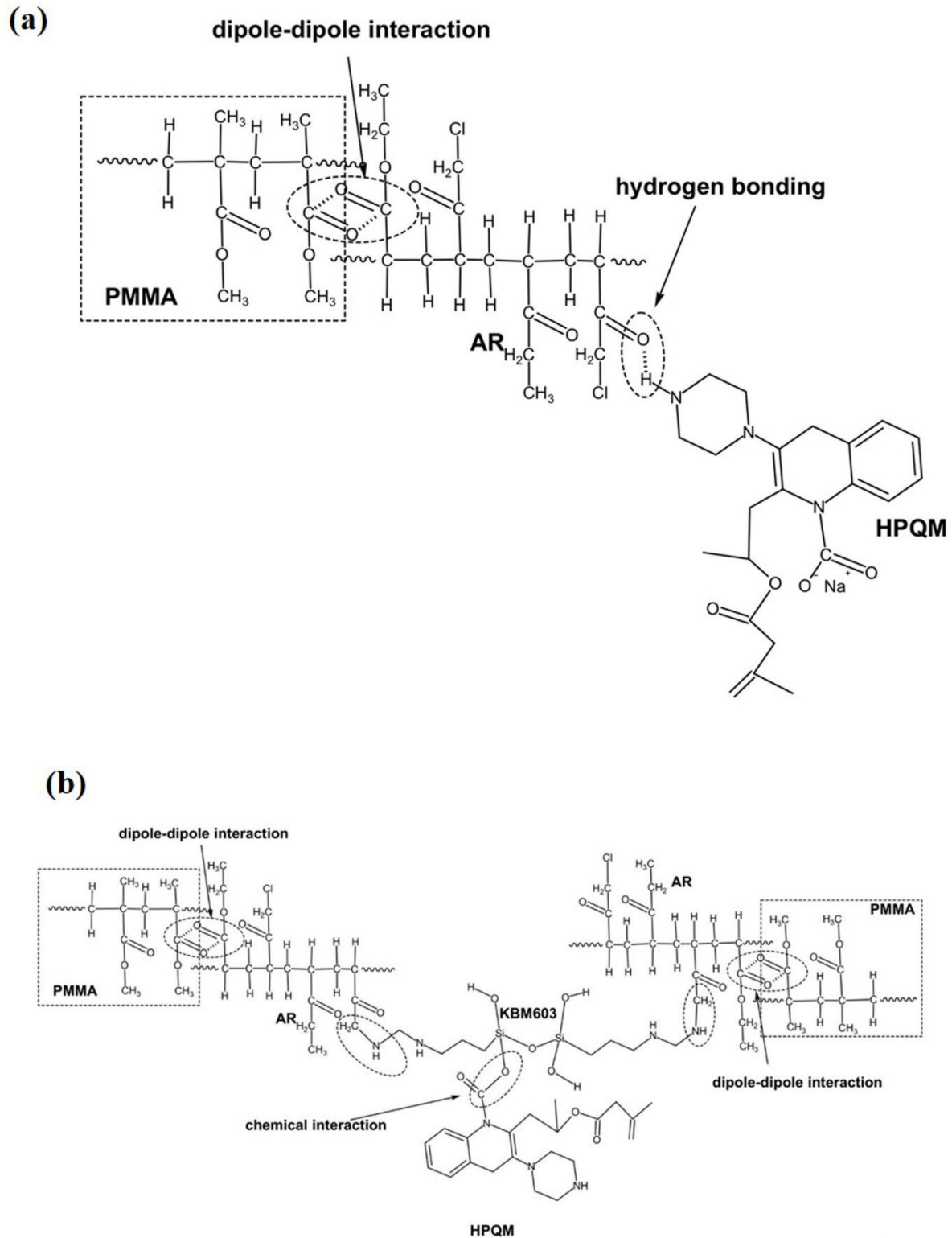
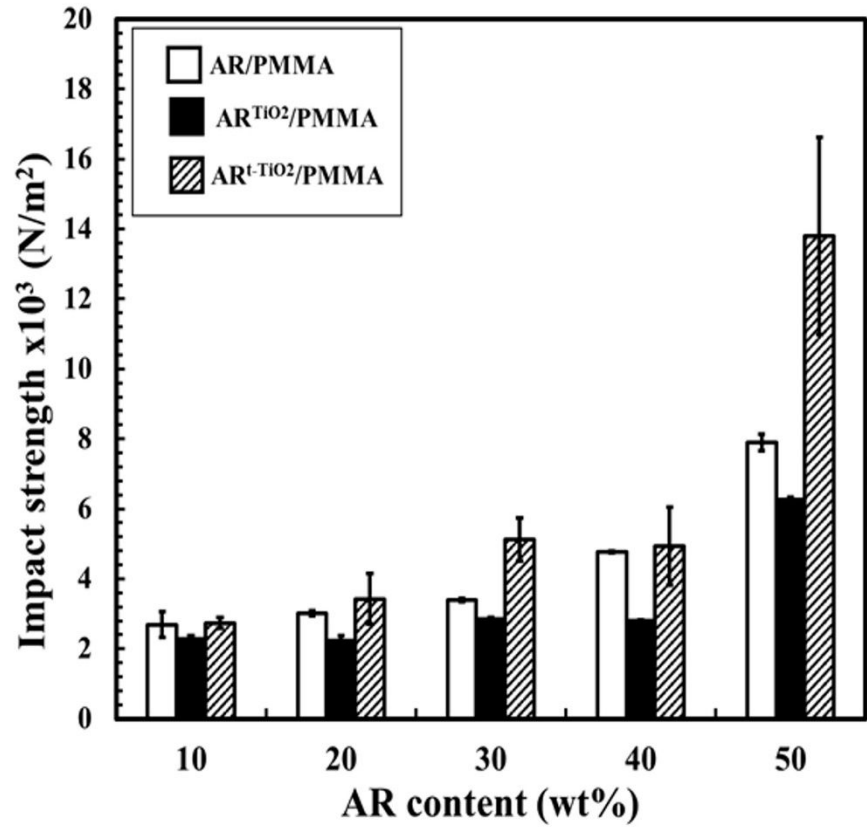


Figure 7 Schematic of the interaction of (a) non-treated and (b) treated HPQM molecule in AR/PMMA blend.

a



b

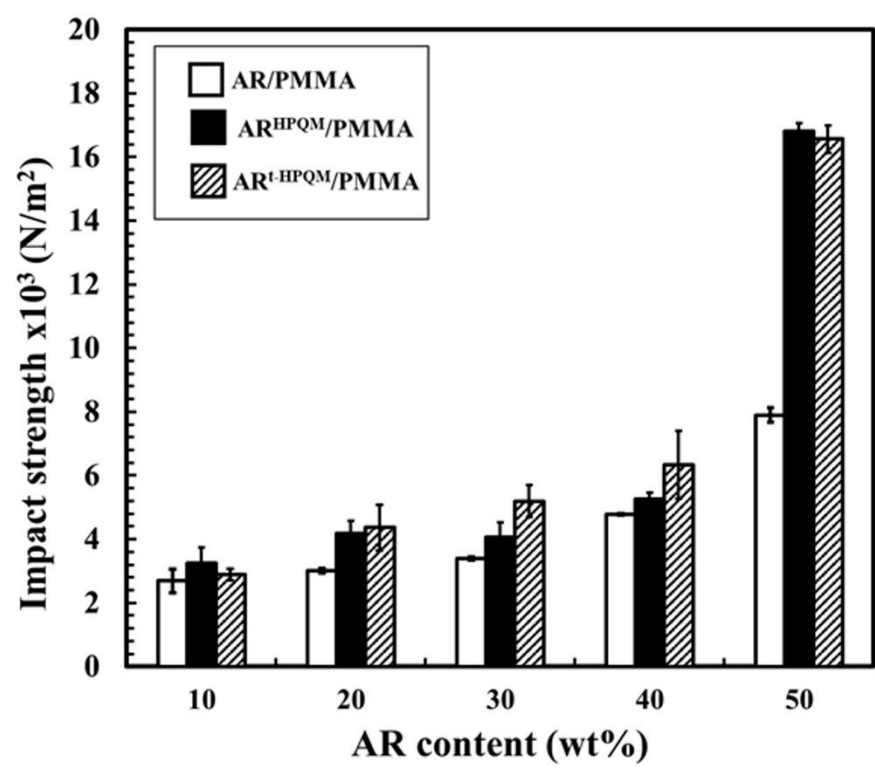


Figure 8 Impact strength of AR/PMMA (white) and AR/PMMA blends with non-treated (black) and treated (pattern) of (a)TiO₂ and (b) HPQM.

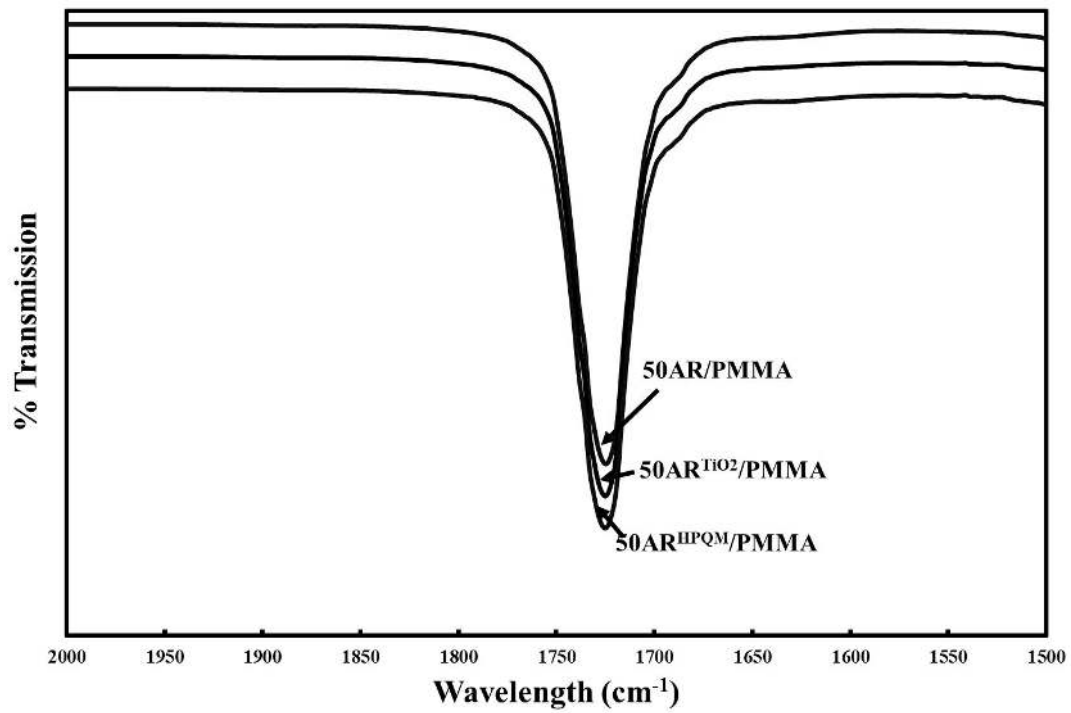


Figure 9 FTIR spectrum of AR/PMMA, AR^{TiO2}/PMMA, and AR^{HPQM}/PMMA in the wavelength range of 1500 to 2000 cm⁻¹.

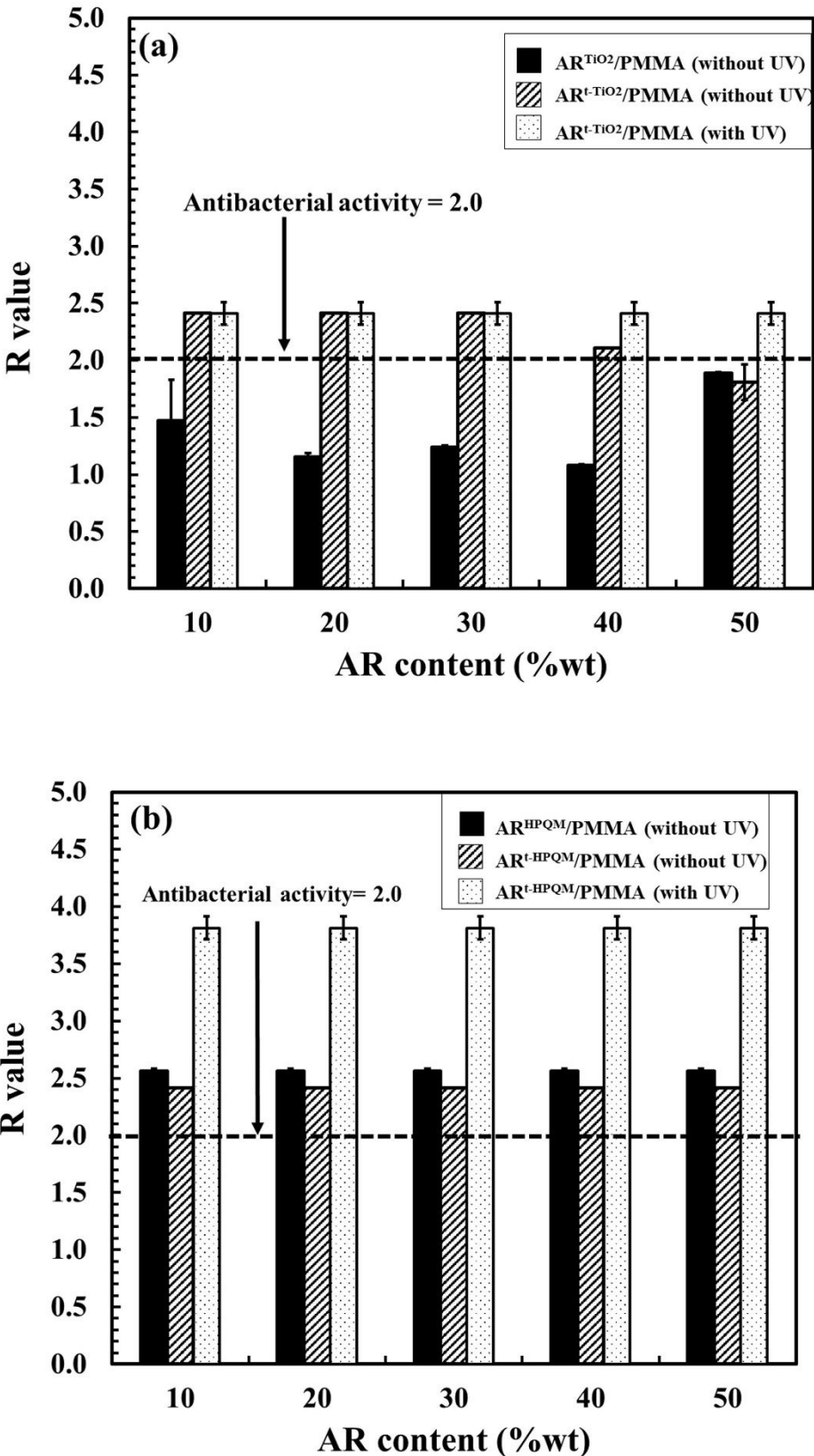


Figure 10 Antibacterial performance of AR/PMMA blends against *E. coli* with non-treated (black) and treated before (gray) and after (white-dot) exposure to UV radiation; (a) TiO₂ and (b) HPQM.